# DEVELOPMENT OF AN ENGINEERING OPTIMIZATION TOOL FOR MINIATURE PULSED PLASMA THRUSTERS

**Igor O. Golosnoy [(1)], Simone Ciaralli [(2)], Stephen B. Gabriel [(3)] , Michele Coletti [(4)]**

*[(1) (3)] University of Southampton, FPSE, ECS, Highfield, Southampton, SO17 1BJ, UK; i.golosnoy@soton.ac.uk , sbg2@soton.ac.uk*
*[(2) (4)] Mars Space Ltd, Unit 61, Basepoint Business Center, Southampton, SO14 5FE, UK; simone.ciaralli@mars-space.co.uk, michele.coletti@mars-space.co.uk*

**KEYWORDS:** electric propulsion, ablative pulsed plasma thruster, modelling

**ABSTRACT:**

Pulsed Plasma Thrusters (PPT) are an established technology for compact thrust propulsion systems. Although PPT optimization has been performed previously it requires complex numerical codes. Although the scaling laws have been suggested they mainly applicable for large thrusters when edge effects can be neglected. A new 0D pulsed inductive acceleration model has been developed which links together the dynamics of the current sheet with the plasma dimensions and ionization processes. The model novelty is in a self-consistent estimation of the plasma sheet properties (temperature, density, thickness) driven by the magnetic pinch pressure and propellant ablation together with its simplicity. Parametric studies have been performed in an attempt to arrive at modified scaling laws for small PPTs.

## 1. INTRODUCTION

It is generally accepted that the discharge evolution of a PPT can be described to a first approximation by a circuit model where the plasma sheet is represented by the discrete and time-constant elements of an RLC series circuit. The circuit model is then coupled with the conservation of the plasma momentum that depends on the discharge current and the inductance change per unit length. This system of equations is called the “snowplow model” [1, 2]. The classic approach in solving it is to assume that all the inputs parameters are constant hence relying on the availability of the experimental data needed to determine the plasma characteristics and the ablated mass. Most of the optimization efforts carried out so far were strongly based on experimental measurements [3-8], although several model of different complexity have been proposed [9-13]. Given the complexity of these processes (coupling of thermal, chemical electromagnetic and gas and plasma dynamics processes), we propose the development of a model where a PPT is represented as an RLC circuit but with electrical parameters that are variable in time and space and obtained from the numerical simulation of the different physical processes hence removing the need of extensive test campaigns. It is important to make the model flexible enough to include edge phenomena which are crucial for small thrust units. The model will have to include: the estimation of the magnetic field generated by the discharge current, the characterization of the plasma column in the discharge (in terms of its size, ionization level, electrons and heavy particle temperature and resistivity) and the quantification of the propellant ablation as a function of the discharge parameters. Assuming a given thruster geometry, we propose an innovative model that will calculate the space and time variable parameters to use as inputs for the standard PPT snowplow model. The snowplow model will then allow for the calculation of the PPT performances in terms of impulse bit, specific impulse and total impulse. By iteratively changing the thruster geometry and input parameters the model can be used to determine the best configuration, intended as the one delivering the highest specific impulse $I_{sp}$ and total impulse, can be selected.

The magnetic field can be calculated in advance from first principle once the thruster geometry is known (assuming a thin current sheet). The propellant ablation model can be derived starting from past modelling efforts [8, 11] or based on semi-empiric relations derived from the analysis of the data available in the literature [14]. A plasma model has developed using simplifying assumptions justified by past experimental observations and supported by the model predictions. This model is based on 3 simplifying assumptions, quasineutrality, full dissociation of PTFE into F and C and that the plasma is in a state of Local Thermodynamic Equilibrium (LTE). A 0D model is developed for plasma motion, solving the conservation of momentum equations and time marching. It is known that substantial amount of ablated material is not ionized due to short dwelling times. The novel model takes into account both plasma and gas components of the impulse bit.

The primary motivation for this work is to develop a simple, but more accurate than the classical models available which rely heavily on empirical data, which is quick to run and would avoid time-consuming, iterative and expensive testing to optimize the design or at least to arrive at a thruster with performance that meets a set of mission requirements. Sophisticated and comprehensive

numerical models like that in [11] are not generally available so the proposed model can be used to find an optimum configuration for a small PPT within a few days computations on laptop PC. It is recommended to run a small number reference tests to confirm assumption on RLC circuit parameters.

The paper is divided into 3 parts. The first describes the model itself while the second is devoted to a comparison of the model results with experimental data from the micro-PPTs built by Mars Space Ltd. in collaboration with the University of Southampton, with the last part presenting some conclusions, scaling laws and brief comments on future work.

## 2. MODEL FRAMEWORK

The overall device model includes sub-models coupled together. We consider

- Electric circuit (coupled with the plasma and motion of the current sheet)
- Plasma properties (coupled to the circuit, ablation, ionization and current sheet)
- Current sheet geometry and motion (coupled to the circuit and plasma properties)
- Ablation (coupled to the plasma and current sheet)

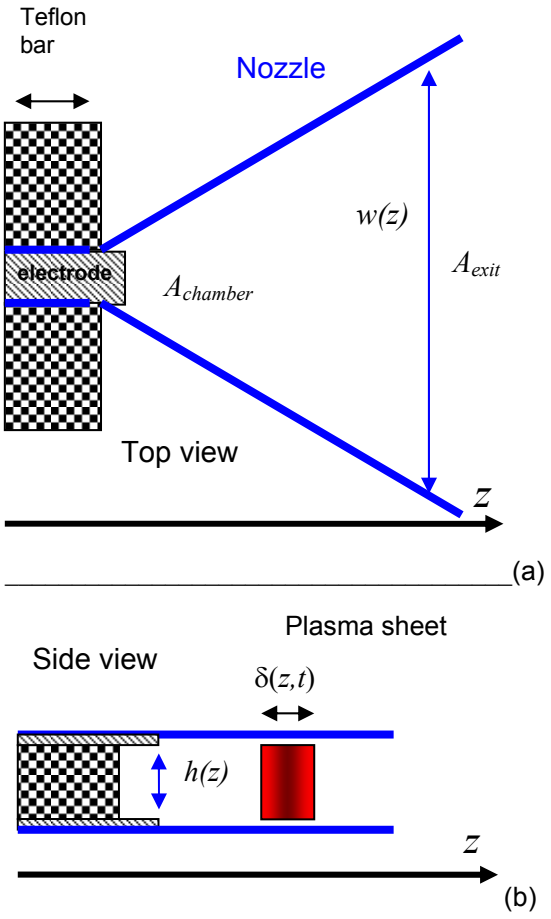


*Figure 1. Model Geometry of PPT chamber.*

### 2.1. Geometry

The schematic of the chamber geometry is given in Fig.1. The chamber forms a nozzle so the gas-dynamic contribution of the thrust can be increased. Also the electrodes are extended beyond the side Teflon blocks to utilize remaining charge on the capacitor for further acceleration of the plasma sheet. The plasma sheet is assumed to be a rectangular with length *h(z)*, width *w(z)* and thickness $\delta(z,t)$ which varies as plasma mass increases due to ablation of Teflon blocks. Both *h* and *w* are fixed by the chamber walls but $\delta(z,t)$ varies to accommodate an ablated mass in the plasma sheet volume, keeping in mind that the plasma density is a function of plasma temperature *T*, pressure *P* and composition (electrons concentration $n_e$, ions concentration $n_i$, average ionization $Z_{av}=n_e/n_i$ and concentration of neutrals $n_0$).

$$\delta(z,t)=\frac{m_p(t)}{\rho(t)h(z)w(z)} \tag{1}$$

For the plasma an ideal gas law is assumed and contribution of electrons to the mass density is ignored with approximate relation is

$$P\approx\left(1+\frac{n_e}{n_i+n_0}\right)\rho\frac{R_gT}{M_{av}},\quad \rho\approx m_h(n_i+n_0) \tag{2}$$

where *P* is plasma pressure, ρ is plasma density, $R_g$ is the universal gas constant, *T* plasma temperature, $M_{av}$ = 16.7 $10^{-3}$ kg/mol is an average molar mass of 33% C – 67% F mixture, $m_h$=16.7 a.u. is an average mass of heavy particle in this mixture.

Classic snowplow model for plasma sheet position *z(t)* is written in the momentum form:

$$\frac{d}{dt}\left(m_pv_p\right)=\frac{1}{2}\frac{dL}{dz}I^2,\ \frac{dz}{dt}=v_p \tag{3}$$

### 2.2. Electric circuit

The discharge is modelled by a simplified LCR circuit:

$$L\frac{dI}{dt}+\left(R+v_p\frac{dL}{dz}\right)I(t)+V(t)=0,\ I=-C\frac{dV}{dt} \tag{4}$$

with total inductance $L=L_d(z)+L_p$, device inductance $L_d(z)$ depends on position of current sheet *z* with $L_d$ (z=0)=18nH, plasma self-inductance is ignored $L_p\approx 0$, resistance is mainly due to plasma with small contribution from electrodes and capacitors bank $R=R_d+R_p$, measured $R_d=5m\Omega$, and resistance of plasma is driven both by plasma conductivity σ and geometry:

$$R_p=\frac{1}{\sigma_p}\frac{h_{eff}}{w_{eff}\delta(z,t)} \tag{5}$$

$$\frac{h_{eff}}{w_{eff}} = \frac{h(z)}{w_{el}} \tag{6}$$

Eq.(6) assumes that the arc mainly burns between the electrodes and an expansion of the are in the middle section can be neglected. In (5) the main contribution comes from *e-i* collisions [15, 16] and for a multi-charged plasma it can be approximated by

$$\sigma_p = 0.4135 \frac{\left(4\pi\varepsilon_0\right)^2 \left(k_B T\right)^{3/2}}{Z_{av} e^2 m_e^{1/2} \ln\Lambda}. \tag{7}$$

where $\varepsilon_0$ is vacuum permittivity, $k_B$ is Boltzman constant, $m_e$ mass of electron, $T$ and $Z_{av}$ is plasma temperature and average ionization respectively, $\ln\Lambda$ is the Coulomb logarithm. The circuit model is coupled with plasma model via conductivity (7) and with geometry via (1).

The current flowing through the plasma sheet creates an average pinch pressure

$$P_p = \frac{\mu_0 I^2}{4w} \tag{8}$$

### 2.3. Plasma properties

In this study plasma Equation of State and kinetic coefficients are taken for LTE conditions. Model estimates for energy transfer time between electrons and ions show that something between 1ns-50ns would be required for the plasma temperatures predicted (maximum relaxation time correspond to the highest predicted temperature 15 eV which drops to 2-4eV at the exhaust plane (end of the discharge chamber, see Section 3). In the experiments since the rise to the maximum temperature value 15 eV takes 500ns to achieve and the electron density is above $10^{23}$ m$^{-3}$, it is believed that plasma will be in LTE, at least approximately. The temperature is assumed to be uniform in the sheet up to the surfaces, $T_i = T_e = T$. This assumption neglects changes in plasma temperature next to the evaporated surface. The plasma composition $n_e(P,T)$, $n_i(P,T)$, $n_0(P,T)$ can be calculated via Saha equation [15],[17] as well as its conductivity eq.(7) and specify enthalpy *H(P,T)*. Although the pressure does vary as the sheet moves in the chamber, it is assumed that on average the pressure is equal to instant pinch pressure (8) plus a small addition to account for gas dynamic pressure in the discharge chamber which is taken as 25000 Pa.

Joule power input in the plasma $I^2 R_p$ results in its heating but a substantial amount of energy is lost to the surfaces and escapes in the form of radiation. Energy flux to the dielectric (Teflon) surface is given in section 2.4, with the radiation being calculated according to Bremsstrahlung only [15, 17]:

$$q_{rad} = 1.57 \cdot 10^{-40} Z_{av}^2 n_e n_i T^{1/2} \tag{9}$$

and overall losses are $Q_{rad} = q_{rad}(wh\delta)$. Losses at the dielectric surface $Q_{diel}$ are given in section 2.4. The processes at the electrodes are complex [15] and their detailed consideration would make the model too complicated. Based on the fact that the predicted plasma temperature reaches ~10eV and above, the main heat flux from the plasma will be generated by bombardment of charged particles on electrodes, i.e.

$$\begin{aligned} Q_{elec} = 2 \cdot \left|\frac{I}{e}\right| \frac{5k_B T}{2} + \\ \left[\left|I_i\right|(V_c + J_{av} - \varphi_{Cu}) - \left|I_e\right|\varphi_{Cu}\right] + \\ \left|I\right|\left[V_a + \varphi_{Cu}\right] \end{aligned} \tag{10}$$

where $\frac{I_e}{I}$ ~0.8, $\frac{I_i}{I}$ ~0.2 are typical fractions of electron and ion cathode currents, $V_a$=12V, $V_c$=12V, $\varphi_{Cu}$=4.5V are anodic, cathodic potential falls, work function for copper [15]. Since the leading effect of pinch pressure (8) is assumed, the energy balance for mass of the sheet $m_p$ is written in an enthalpy form with *H* being an enthalpy per unit mass:

$$\frac{d}{dt}\left(m_p H\right) = I^2 R_p + \delta w h \frac{dP}{dt} - Q_{rad} - Q_{diel} - Q_{elec} \tag{11}$$

### 2.4. Teflon ablation

The ablation model is based on [8] with additional simplifications as discussed below. Particles fluxes to PTFE surfaces from plasma can be expressed as

$$\begin{aligned} \varphi_e &= \frac{1}{4} n_e \left(\frac{8k_B T}{\pi m_h}\right)^{1/2}, \\ \varphi_i &= \frac{\varphi_e}{Z_{av}}, \\ \varphi_0 &= \frac{1}{4} n_0 \left(\frac{8k_B T}{\pi m_h}\right)^{1/2} \end{aligned} \tag{12}$$

Electrons slow down due to the sheath with potential

$$\phi = \left(\frac{k_B T}{2e}\right) \ln\left(\frac{m_h}{m_e}\right) \tag{13}$$

They lose energy on impact with the surface and deposit at the top layer.

$$q_e = \varphi_e a_e 2k_B\left(T - T_s\right),$$
$$q_i = \varphi_i a_i\left[2k_B\left(T - T_s\right) + Z_{av} e\phi\right], \quad (14)$$
$$q_0 = \varphi_0 a_0 2k_B\left(T - T_s\right)$$

Energy accommodation coefficients of electrons, ions and neutrals $a_e$, $a_i$, $a_0$ can be expressed in terms of the mass ratio of incoming particle and an average mass of atom in PTFE:

$$a_x = \frac{2\mu_x}{\left(1+\mu_x\right)^2}, \mu_x = \frac{m_x}{m_h} \quad (15)$$

Effectively, for heavy particle $a$=0.5 and it can be neglect for electrons. The ablation flux is driven by Langmuir's relation [18]:

$$\Gamma = \left(\frac{m_h}{2\pi k_B T_s}\right)^{1/2} P_{vap} \quad (16)$$

The vaporization pressure of PTFE is

$$P_{vap} = P_c \exp\left(-\frac{T_c}{T_s}\right) \quad (17)$$

where $P_c$ = 1.84×10$^{15}$ Pa , $T_c$ = 20815 K and $T_s$ is PTFE surface temperature.

On the surface the energy input from particles impacts and radiation is balanced by energy losses to evaporation (low thermal diffusivity of PTFE and short exposure times allows to neglect heating of PTFE bulk):

$$q_i + q_e + q_0 + q_{rad} = q_{abl} \quad (18)$$

$$q_{abl} = \Gamma\left(\frac{2k_B T_s}{m_h} + H_{pol} + H_{ev}\right) \quad (19)$$

where $H_{pol}$ = 1.58 MJ/kg, and $H_{ev}$ = 25 MJ/kg are polymerization and evaporation enthalpies of PTFE [19-21]. Value of $H_{ev}$ has been increased by a factor of 2 in comparison with [19] but consistent with [20, 21] and incorporates dissociation effects since only an atomic (no molecules) gas-plasma mixture is considered in Saha model.

Equations (12)-(19) are solved with known plasma properties to find the self-consistent propellant surface temperature $T_s$.

### 2.5. Ionization of ablated material

Under intensive evaporation neutral atoms enter the plasma near the surface region where electron ionization capabilities are reduced due to slowdown in the sheath. To find the ionization frequency a standard classical formula [17] is utilized (average ionization threshold $J_{av}$=15.7eV and Maxwell velocity distribution of electrons have been assumed):

$$\chi_{ion} = \frac{\pi e^4}{\left(4\pi\varepsilon_0\right)^2 J_{av}^2} u_e n_e \exp\left(-\frac{J_{av}}{k_B T}\right) \quad (20)$$

with the average velocity of electrons corrected for the deceleration in the pre-sheath:

$$u_e = \left(\frac{8k_B T}{\pi m_e}\right)^{1/2}\left(\frac{m_e}{m_h}\right)^{1/2} \quad (21)$$

The fraction of ionized atoms increases with time according to

$$n_{ion}(t)/n_{at}(t=0) = \left(1 - \exp(-\chi_{ion} t)\right) \quad (22)$$

but the atoms entering the sheet at different points stay within the hot region for different times. Integration over the dwelling time up to the max $\Delta t_{\max} = z/v_p$ results in the mass entering the sheet being given by:

$$\frac{dm_p}{dt} = \frac{dm_{abl}}{dt}\left(1 - \frac{v_p}{\chi_{ion}\delta}\exp\left(-\frac{\chi_{ion}\delta}{v_p}\right)\right) \quad (23)$$

$$\frac{dm_{abl}}{dt} = \delta h \Gamma\,, \quad \frac{dm_{gas}}{dt} = \frac{d\left(m_{abl} - m_p\right)}{dt} \quad (24)$$

where $m_{abl}$ is the overall ablated mass, and $m_p$ is the addition to the plasma sheet. In (23)-(24) the presence of neutrals within the plasma sheet is ignored since the temperature exceeds 10000 K.

### 2.6. Solution method

The model has been implemented in COMSOL commercial software and solved using a fully coupled solver. The time step was taken to be 1ns to capture fast changes in plasma properties. To check for convergence, the time step was reduced to 0.5ns and 0.1ns and it resulted in less than 5% variations in the model outputs. The plasma parameters and exhaust velocity are calculated at the edge of the discharge chamber. Further expansion through the nozzle is approximated by analytical formulas tabulated in [22].

When the current sheet reaches the end of electrodes it is assumed that the arc continues to burn at the fixed position until it naturally decays as the current drops.

## 3. MODEL VERIFICATION

The model predictions have been compared with experimental measurements done on the setup schematically presented on Figure 1. The nozzle area ratio was around 4. The capacitor stored

energy was 2 J. It is assumed that after the initial spark at 8200K ablated a mass of $10^{-2}$ μg (the model is insensitive to these inputs). Short electrodes was used in the study. The comparison is given in Table 1 (see Appendix) for various geometries. Overall, the model agrees with the measured integral quantities within 10% for ablated mass and within 20% for specific impulse. Of course such oversimplified model based on global energy balance cannot capture all details of plasma-gas expansion and it should be used as a qualitative design tool.

The model predicts the peaking of electrons temperature above 10 eV at the beginning of the discharge and it drops to 2-3 eV at the end of the pulse. The second peak current at the second half of the first cycle gives a slight rise of the temperature, Figure 2. Such behaviour is consistent with Langmuir probe measurements [23].

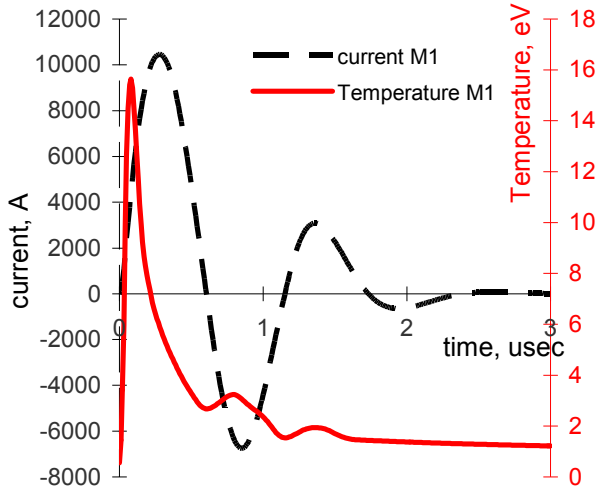


*Figure 2. Example of the predicted current waveform.*

## 4. PARAMETRIC STUDIES

A set of design parameters has been varied to demonstrate the model capabilities. The model was used for the case of short electrodes, when the arc continues to ablate propellant until a complete discharge of the capacitor bank. 2 parameters were concentrated on: the height of the discharge chamber (distance between electrodes), and the length of the Teflon bars (it gives higher propellant area / discharge chamber cross-section ratio).

An increase in the height of the chamber results in a larger surface area of Teflon exposed to the plasma which in turn would give a higher mass bit but reduces the current (via increased plasma resistance). In spite of reduction in current, the temperature follows very similar trend because smaller volume to surface ration in the extended chamber reduces thermal losses. In the first 0.2-0.3 μs after the initiation the ablation rates are very similar (Figure 3) but larger channel produces higher ablation rates afterwards. The ionization rate is a strong function of temperature and the plasma is produced within 1 μs. Actually electromagnetic acceleration is applied to a fraction of the ablated material (~40-50%) and late ablation only contributes to the thermal part of the impulse, which in turn reduces the efficiency of the thruster. The late ablation contribution is higher for larger height, see Figure 3 and Table 1. It may appear that the distance between the electrodes should be as small as possible. But of course, a small height brings excessive thermal losses to the electrodes and ablation rate is low as well as the impulse bit. So the optimal height does exist, it reduces the ablation mass to a reasonable limit, results in higher acceleration and shorter ablation duration. Such optimal configuration corresponds to a minimal possible chamber height which delivers the required impulse bit. It can be found by a trial and error method using the model.

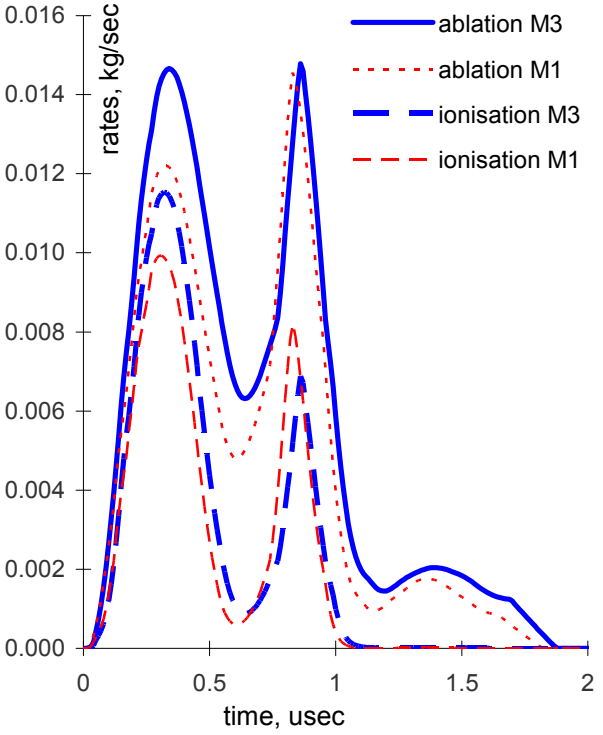


*Figure 3. Ablation and ionisation rate as a function of the chamber height.*

An increase in the electromagnetic part of the impulse can be achieved by increasing the propellant bar (and the discharge chamber) length rather than height. In this case the initial current waveform is unaffected and the electromagnetic part of the impulse increases as the sheet continues to accelerate along the electrodes, Table 1. Nevertheless thermal part of the impulse increases to greater extends due to lower plasma temperature at the chamber exit, Table 1. It is interesting to note the effects of propellant edges on the ablation. Double peak for the ablation rate in M2 (Figure 4) corresponds to the motion of the sheet along the edge of the bars. The first maximum is due to maximum current in the second half-cycle. The next ablation peak occurs at lower current when the sheet leaves the chamber and the arc continues to burn at the edges of the bars. It indicates a strong correlation of the thruster characteristics and the design features, including mutual arrangements for electrodes and propellant bars. It also suggests that there is an optimal bars' length. The increase in the propellant area result in the increase in the

ablated mass and at the final stages of the discharge the ionization rate drops due to lower temperature. So the mass increase does not translate into the proportional increase of $I_{bit}$, since the electromagnetic part of the impulse increases less than expected. But shorter length with small ablated mass ejects plasma sheet very quickly and mainly contributes to thermal part of the impulse. So the optimal length does exist, it produces enough ablation mass to keep the discharge within the chamber while the current flows. Such optimal configuration can be found by a trial and error method using the model.

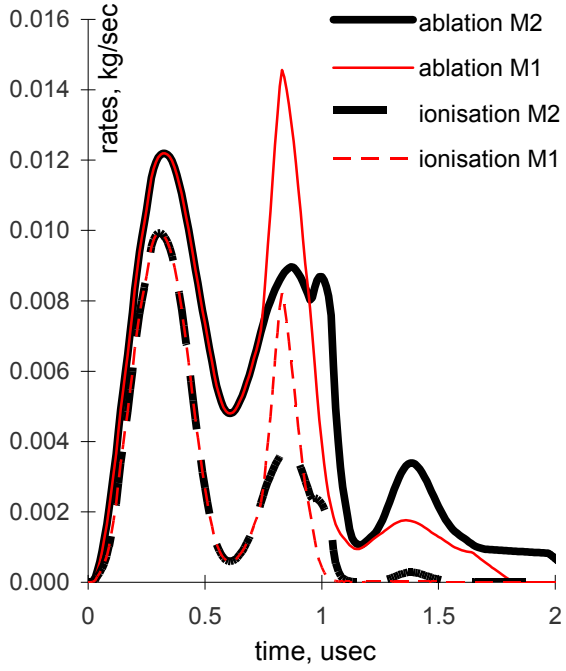


*Figure 4. Ablation and ionisation rate as a function of the chamber length.*

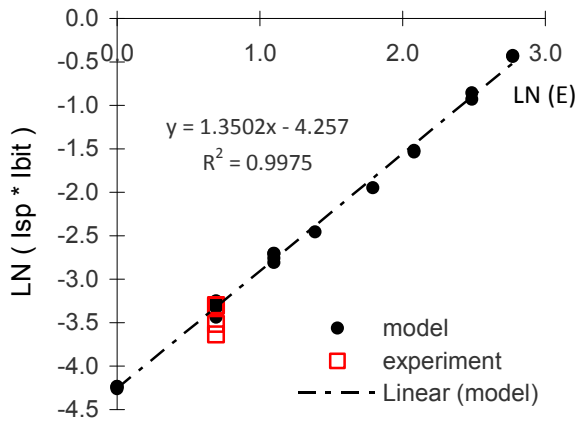


*Figure 5. Scaling law for the* product $I_{bit}\, I_{sp}$.

Various scaling laws have been suggested to assist in ablative PPT design. They summarised in [24]. It was found that the ablated mass depend on the ratio of Propellant area / Discharge chamber cross-section ($A_p / A_{ex}$) and the current action integral which in tern is a function of the discharge energy $E$. Specific impulse was shown to be a power function of the ratio $E / A_p$ , whereas product $I_{bit}\, I_{sp}$ depends only on energy $E$. To investigate the scaling laws for small PPT discharge energy was varied and also the models' geometries M1, M2, M3, M4 were extended by factor of two to observe changes in the performance.

It is confirmed that $I_{bit}\, I_{sp}$ depends only on energy $E$, see Figure 5.

$$I_{bit} I_{sp} \sim E^{1.35} \qquad (25)$$

The product increases with the energy but the exponent is lower than reported in [24] (1.35 vs 1.6). It indicates bigger losses in small ablative PPTs in comparison with larger units.

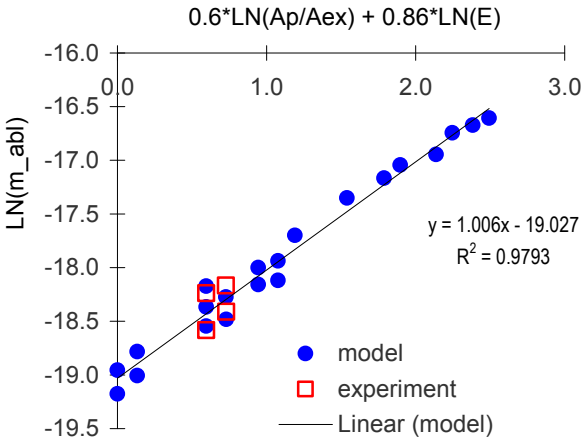


*Figure 6. Scaling law for the ablated mass.*

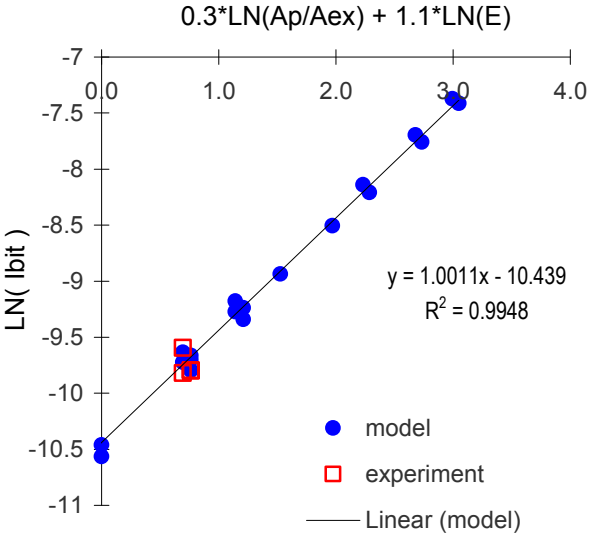


*Figure 7. Scaling law for $I_{bit}$.*

The ablated mass can be approximated by eq.(26)

$$m_{abl} \sim \left( \frac{A_p}{A_{ex}} \right)^{0.6} E^{0.86}, \qquad (26)$$

whereas the impulse

$$I_{bit} \sim \left( \frac{A_p}{A_{ex}} \right)^{0.3} E^{1.1}, \qquad (27)$$

The relation eq.(27) is different from the previously reported $E / A_p$ , dependence and it is clear that the impulse is influenced by the energy and the geometry differently (energy has much greater influence). Although it is generally expected that both mass and impulse are proportional to the discharge energy, it is not strictly correct as can be seen from eqs.(26),(27).

## 5. CONCLUSIONS

It was shown that a simple 0D pulsed inductive acceleration model can be successfully used to optimize ablative PPT design. A key feature of the model is a self-consistent consideration of the plasma properties and the ablation process. It was shown that a required impulse bit can be achieved by varying the geometries of the propellant bars (height vs width) while keeping their cross-sectional areas (and their masses) constant. Additional increase of the impulse can be obtained by increasing the length of the discharge chamber. But in this case the increase is mainly due to thermal part of the impulse and the efficiency of such PPT is reduced. An impulse bit above 50 μN·s per 2 J shot can be achieved with a specific impulse of around 500 s. The future work will include extended parametric studies, assembly and testing of several PPTs with most promising configurations, which will aid in further validation of the model.

## 6. ACKNOWLEDGMENTS

This work has been supported by EPSRC via grant EP/M506783/1 and by TSB via grant 101884.

## 7. REFERENCES

[1] M. Andrenucci, Magnetoplasmadynamic Thrusters, Encyclopedia of Aerospace Engineering: *John Wiley & Sons*, 2010.

[2] R. Jahn, Physics of Electric Propulsion. *New York: McGraw-Hill*, 1968.

[3] D. J. Palumbo and W. J. Guman, Effects of Propellant and Electrode Geometry on Pulsed Ablative Plasma Thruster Performance, *Journal of Spacecraft and Rockets*, vol. 13, pp. 163-167, 1976.

[4] R. J. Vondra and K. I. Thomassen, Performance Improvements in Solid Fuel Microthrusters, *Journal of Spacecraft and Rockets*, vol. 9, pp. 738-742, 1972.

[5] N. Schonborg and S. Hornfeldt, Model of the temperature dependence of the hysteresis losses in a high-temperature superconductor, *Physica C*, vol. 372, pp. 1734-1738, 2002.

[6] T. Schonherr and e. al, Influence of Electrode Shape on Performances of Pulsed Magnetoplasmadynamic Thruster SIMPL-LEX, *Journal of Propulsion and Power*, vol. 25, pp. 380-386, 2009.

[7] H. Tahara, Y. Ishii, M. Tanaka, M. Naka, and Y. Watanabe, Flowfield Calculation of Electrothermal Pulsed Plasma Thrusters for the PROITERES Satellite, presented at the 32nd International Electric Propulsion Conference, Wiesbaden, Germany, 2011.

[8] T. Edamitsu and H. Tahara, Performance Measurement and Flowfield Calculation of an Electrothermal Pulsed Plasma Thruster With A Propellant Feeding Mechanism, presented at the 29th International Electric Propulsion Conference, 2005.

[9] K. A. Polzin, K. Sankaran, A. G. Ritchie, and J. P. Reneau, Inductive pulsed plasma thruster model with time-evolution of energy and state properties, *J. Phys. D: Appl. Phys.*, vol. 46, p. 475201 (14pp), 2013.

[10] M. Keidar and I. D. Boyd, Ablation Study in the Capillary Discharge of an Electrothermal Gun, *Journal of Applied Physics*, vol. 99, p. 053301, 2006.

[11] M. Keidar, I. D. Boyd, E. L. Antonsen, R. L. Burton, and G. G. Spanjers, Optimization Issues for a Micropulsed Plasma Thruster, *Journal of propulsion and power*, vol. 22, pp. 48-55, 2006.

[12] M. Keidar, I. D. Boyd, and I. I. Beilis, Electrical Discharge in the Teflon Cavity of a Coaxial Pulsed Plasma Thruster, *IEEE Transactions on Plasma Science*, vol. 28, pp. 376-385, 2000.

[13] M. Keidar, I. D. Boyd, and I. I. Beilis, Ionization and Ablation Phenomena in an Ablative Plasma Accelerator, *Journal of Applied Physics*, vol. 96, pp. 5420-5428, 2004.

[14] M. Keidar and e. al, Analyses of Teflon Surface Charring and Near Field Plume of a Micro-Pulsed Plasma Thruster, presented at the 27th International Electric Propulsion Conference, 2001.

[15] Y. P. Raizer, Gas Discharge Physics. *Berlin: Springer-Verlag*, 1981.

[16] E. M. Lifshitz and L. P. Pitaevskii, Physical Kinetics: Volume 10 (Landau and Lifshitz: Course of Theoretical Physics). *Oxford: Pergamon Press*, 1981.

[17] B. M. Smirnov, Plasma Processes and Plasma Kinetics: *WILEY-VCH Verlag*, 2007.

[18] M. Keidar, I. D. Boyd, and I. I. Beilis, Model of an Electrothermal Pulsed Plasma Thruster, *Journal of Propulsion and Power*, vol. 19, pp. 424-430, 2003.

[19] C. Ruchti and L. Niemeyer, Ablation Controlled Arcs, *IEEE Trans. Plasma Sci.*, vol. PS-14, pp. 423-434, 1986.

[20] T. Christen, A maximum entropy production model for Teflon ablation by arc radiation, *J Phys D: Appl. Phys*, vol. 40, pp. 5719-5722, 2007.

[21] M. Seeger, J. Tepper, T. Christen, and J. Abrahamson, Experimental study on PTFE ablation in high voltage circuit-breakers, *J Phys D: Appl. Phys,* vol. 39, pp. 5016–5024, 2006.

[22] J. D. Anderson, Fundamentals of Aerodynamics: *McGraw-Hill*.

[23] N. A. Gatsonis, L. T. Byrne, J. C. Zwahlen, E. J. Pencil, and H. Kamhawi, Current-Mode Triple and Quadruple Langmuir Probe Methods With Applications to Flowing Pulsed Plasmas, *IEEE Transactions on Plasma Science*, vol. 32, pp. 2118-2129, 2004.

[24] R. L. Burton and P. J. Turchi, Pulsed Plasma Thruster, *Journal of Propulsion and Power*, vol. 14, pp. 716-735, 1998.

Appendix.

*Table 1. Predicted dependence of PPT performance compared with measured characteristics as a function of discharge chamber dimensions. Energy in the capacitor bank is 2 J.*

| ***Experiment (E) / Model (M)*** | **E1** | **M1** | **E2** | **M2** | **E3** | **M3** | **E4** | **M4** |
|---|---|---|---|---|---|---|---|---|
| Propellant area / Discharge chamber cross-section | 1.0 | 1.0 | 1.25 | 1.25 | 1.0 | 1.0 | 1.25 | 1.25 |
| Height / Width | 2.0 | 2.0 | 2.0 | 2.0 | 2.8 | 2.8 | 2.8 | 2.8 |
| **Total ablated mass, μg** | **8.5 ± 0.1** | **8.8** | **10.1 ± 0.1** | **9.4** | **12.0 ± 0.1** | **10.6** | **12.9 ± 0.1** | **11.6** |
| Mass of current sheet (ionised), μg | | 4.2 | | 4.0 | | 4.7 | | 4.5 |
| **Total Impulse bit, μN·s** | **55.4 +/- 5.0** | **55.7** | **54.4 +/- 4.9** | **59.8** | **55.8 +/- 5.0** | **61.3** | **68.2 +/- 6.1** | **65.4** |
| Electromagnetic part of impulse, μN·s | | 48.1 | | 51.0 | | 51.8 | | 54.0 |
| Thermal part of impulse, μN·s | | 7.5 | | 8.8 | | 9.5 | | 11.4 |
| **Specific impulse total, s** | **663 +/- 60** | **642** | **547 +/- 50** | **648** | **473 +/- 43** | **593** | **540 +/- 49** | **576** |

MARS SPACE LTD
SPACE AND PLASMA TECHNOLOGIES

UNIVERSITY OF Southampton
School of Electronics and Computer Science

# Development of a modelling optimization tool for miniature pulsed plasma thrusters

Igor Golosnoy and Stephen Gabriel*
Simone Ciaralli and Michele Coletti**
* University of Southampton, UK
** Mars Space Ltd, UK

MARS SPACE LTD
SPACE AND PLASMA TECHNOLOGIES

# Motivation

UNIVERSITY OF Southampton
School of Electronics and Computer Science

- Simple tool for qualitative performance evaluation of small pulsed plasma thrusters
  - Suitable for parametric studies
  - Qualitative model to guide experimental design
- Specific issue related to the size scale
  - Volume to surface ratio is significantly less vs larger units
  - Importance of edge phenomena and surface effects

MARS SPACE LTD
SPACE AND PLASMA TECHNOLOGIES

# Outcomes

UNIVERSITY OF Southampton
School of Electronics and Computer Science

- Jumping ahead …
  - Modifications of scaling laws
  - Different design parameters

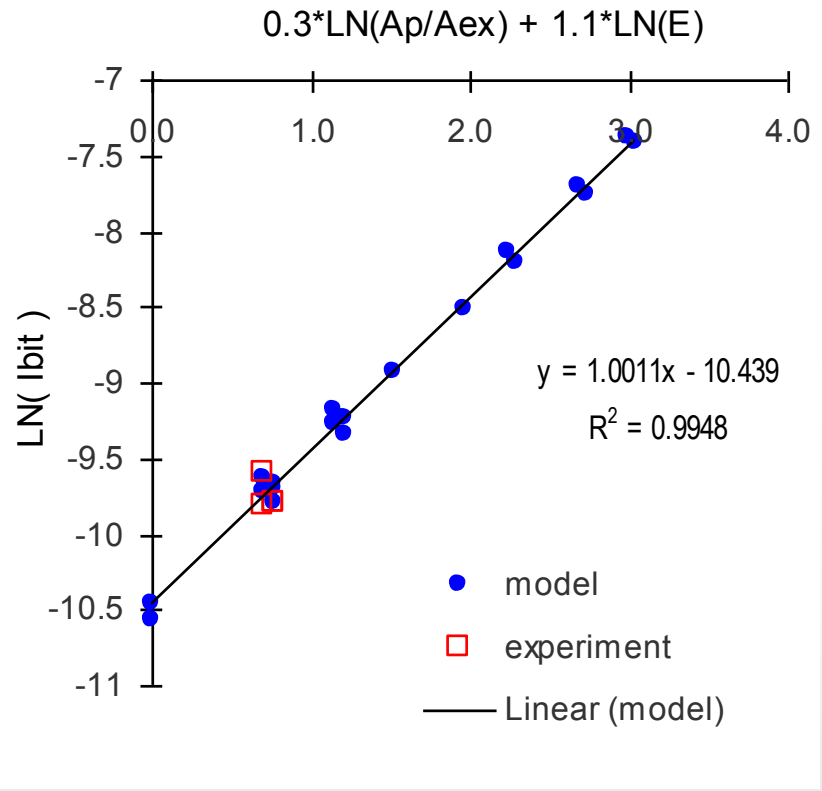


R. L. Burton and P. J. Turchi, Pulsed Plasma Thruster, *Journal of Propulsion and Power*, vol. 14, pp. 716-735, 1998.

$$I_{bit} : A_p^{0.6} E^{1.0}$$

$$I_{bit} : \left(\frac{A_p}{A_{ex}}\right)^{0.3} E^{1.1}$$

MARS SPACE LTD

SPACE AND PLASMA TECHNOLOGIES

UNIVERSITY OF Southampton

School of Electronics and Computer Science

# Geometry

MARS SPACE LTD
SPACE AND PLASMA TECHNOLOGIES

# Subject

UNIVERSITY OF Southampton
School of Electronics and Computer Science

- Pulse Plasma Thrusters
  - Solid (Teflon)
  - Side-fed
- Simple operational principle
- But complex coupled physics
  - Power supply (current) – arc phenomena – plasma generation – surface evaporation – magnetohydrodynamics
- It is not easy to optimize
  - Existing devices can be improved by simulation of couple phenomena

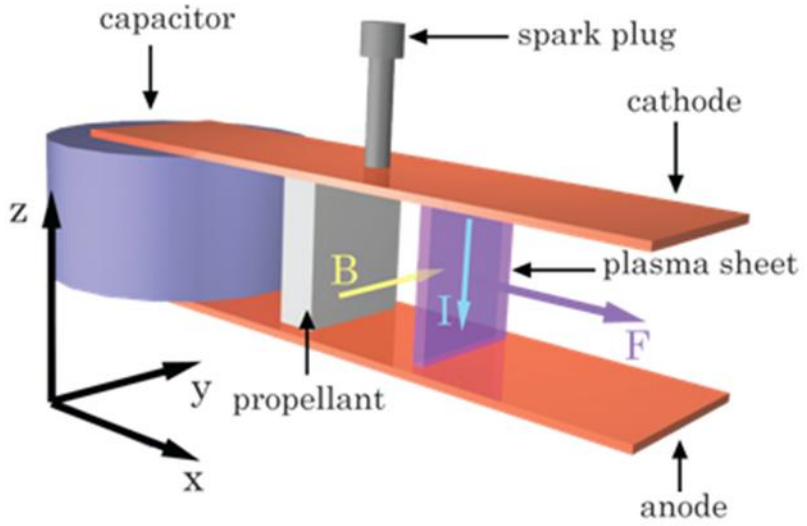


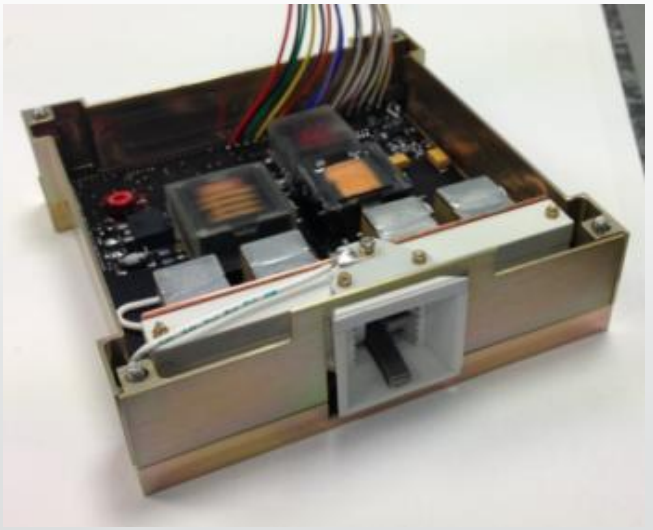

MARS SPACE LTD
SPACE AND PLASMA TECHNOLOGIES

# Geometry of PPT chamber

UNIVERSITY OF Southampton
School of Electronics and Computer Science

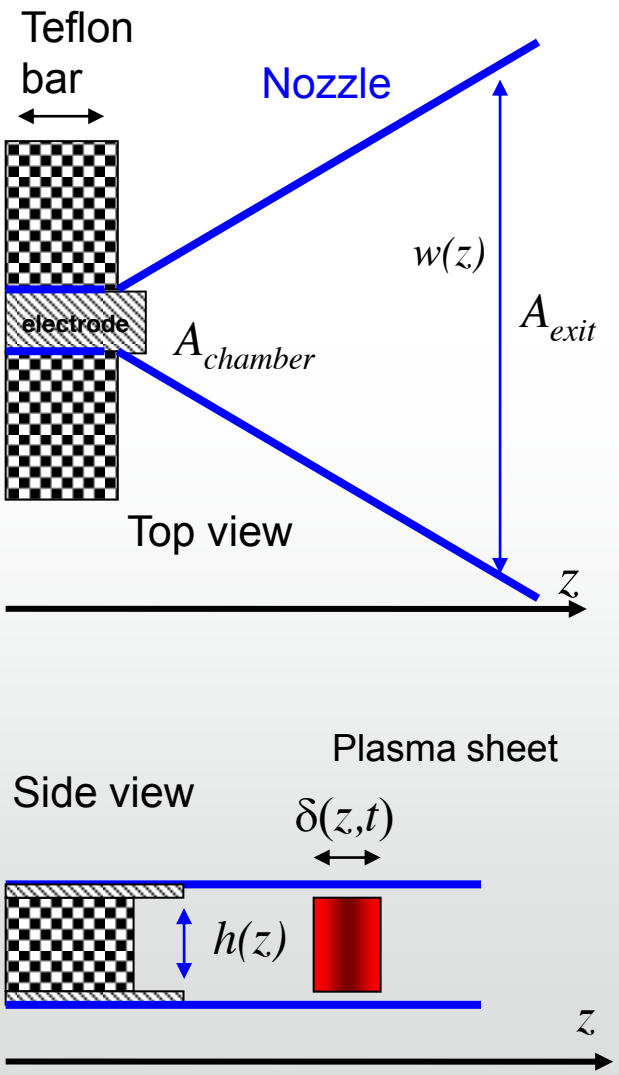


- Model flexibility
  - Section properties varies with position z
  - Connecting point (bar edge, electrodes, nozzle start point) can be given a special consideration

MARS SPACE LTD
SPACE AND PLASMA TECHNOLOGIES

UNIVERSITY OF Southampton
School of Electronics and Computer Science

# Model Framework

MARS SPACE LTD
SPACE AND PLASMA TECHNOLOGIES

# Framework

UNIVERSITY OF Southampton
School of Electronics and Computer Science

- Snowplow formulation
- Energy balance
  - Coupled with electric circuit
  - Plasma is a variable resistor
  - Losses at electrodes and propellant surfaces
  - Radiation
- Electromechanical conversion described via inductance variations
  - Momentum transfer
  - e.m.f in the load circuit
- Ablation
  - Langmuir's model
- Ionisation
  - Only a fraction of ablated mass is ionised

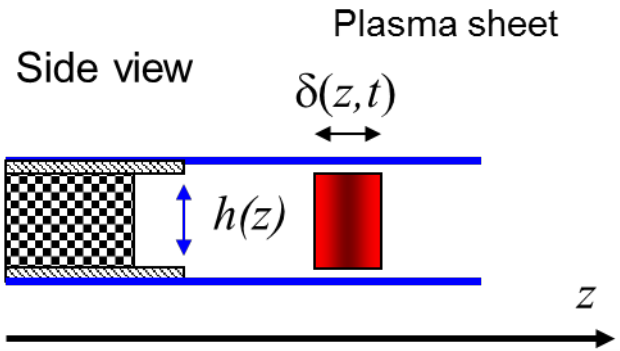

MARS SPACE LTD
SPACE AND PLASMA TECHNOLOGIES

# Plasma model

UNIVERSITY OF Southampton
School of Electronics and Computer Science

- How to predict ionisation level?
  - Local Thermal Equilibrium
  - Pinch pressure plus small gas dynamics contribution
  - Saha equation
- LTE is valid only appropriate at initial stages
  - Assumption for qualitative analysis
  - Predicted composition ($C^{4+}$ ions) is consistent with experiments
- Mass of ionised fraction
  - Subroutine for ionisation kinetics

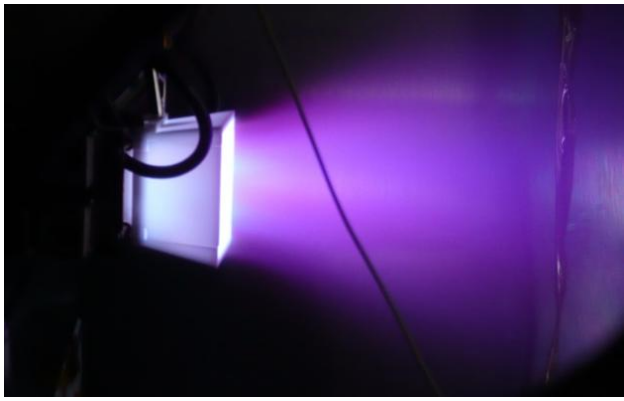

# Surface Phenomena



- Attachment to cathode and anode
  - Significant energy losses
- Propellant ablation
  - Inner sides, Edges, Outer surfaces

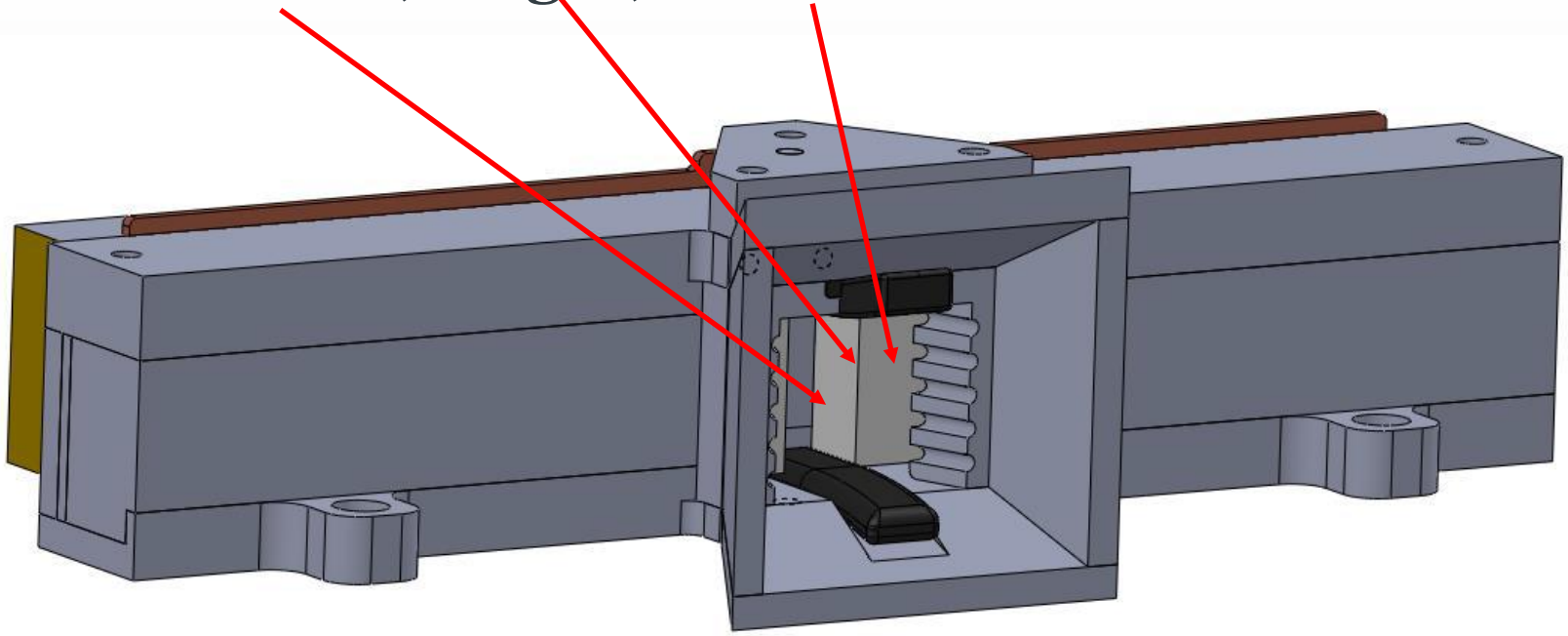

MARS SPACE LTD
SPACE AND PLASMA TECHNOLOGIES

UNIVERSITY OF Southampton
School of Electronics and Computer Science

# Examples

MARS SPACE LTD
SPACE AND PLASMA TECHNOLOGIES

# Depth

UNIVERSITY OF Southampton
School of Electronics and Computer Science

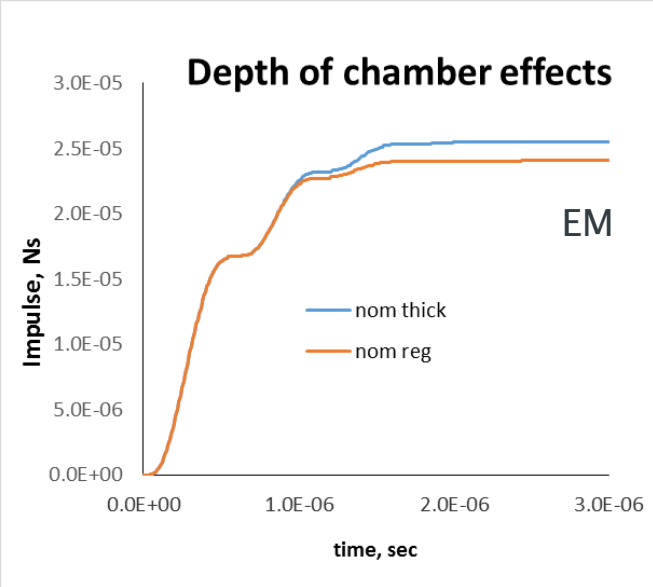


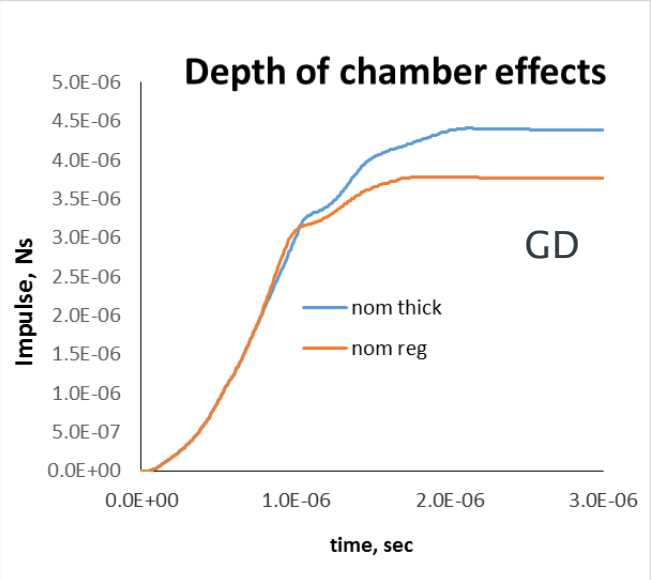


$I_{EM}$ – only small increase
$I_{GD}$ – noticeable increase

But $I_{EM} >> I_{GD}$

Why?
$d_1 < d_2$
$m_1 < m_2$

but
$m_{1ionised} \sim m_{2ionised}$

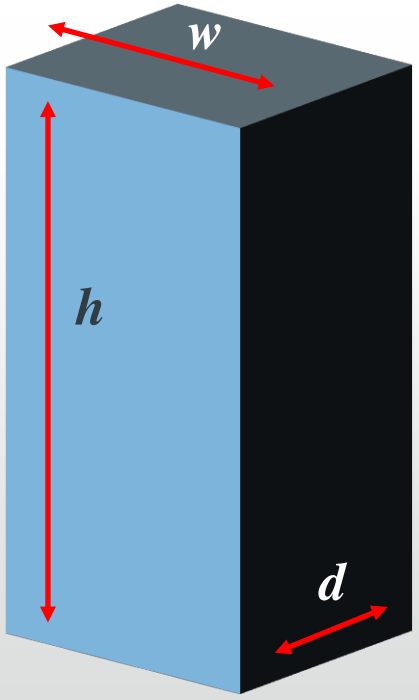

MARS SPACE LTD
SPACE AND PLASMA TECHNOLOGIES

# Depth

UNIVERSITY OF Southampton
School of Electronics and Computer Science

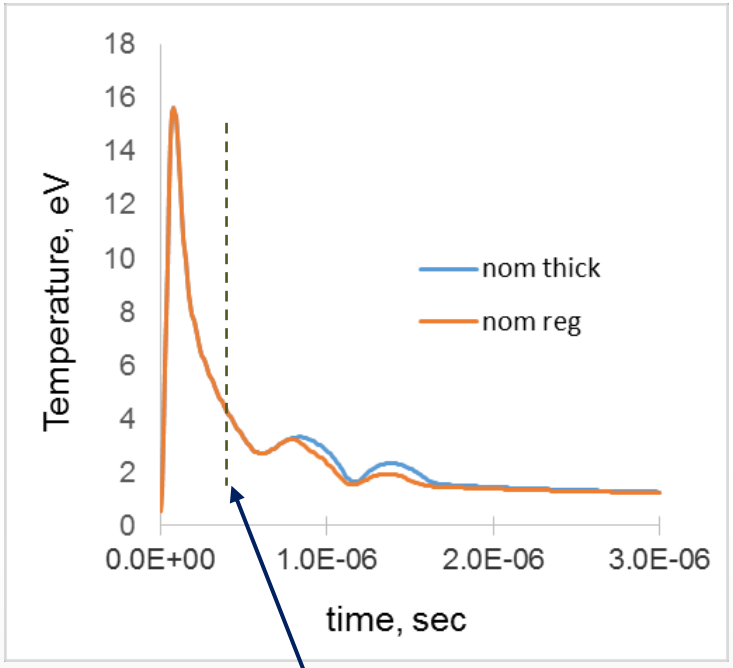


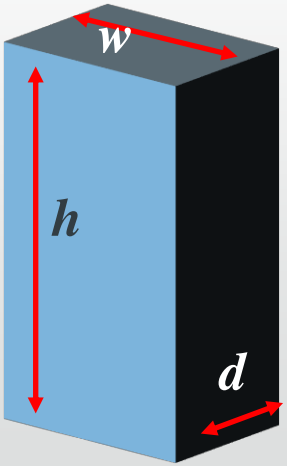


Late ablation: Very little ionisation

Very shallow chamber?

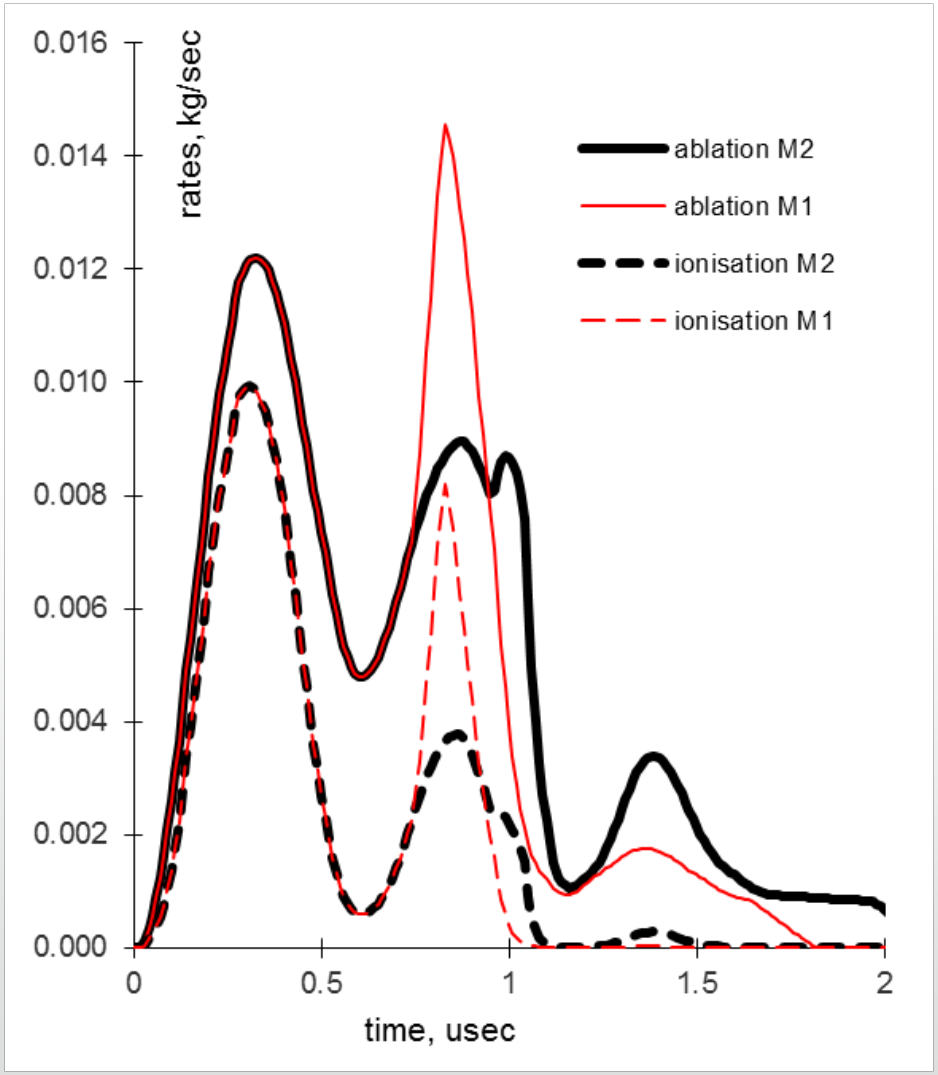

MARS SPACE LTD
SPACE AND PLASMA TECHNOLOGIES

# Height

UNIVERSITY OF Southampton
School of Electronics and Computer Science

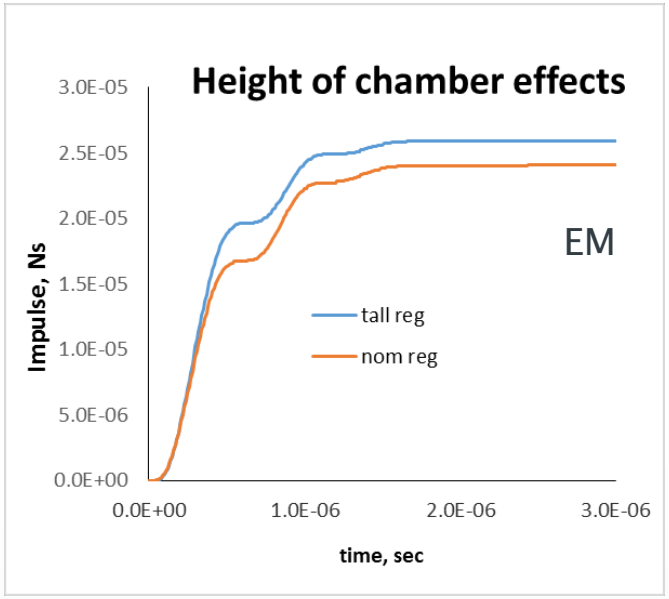


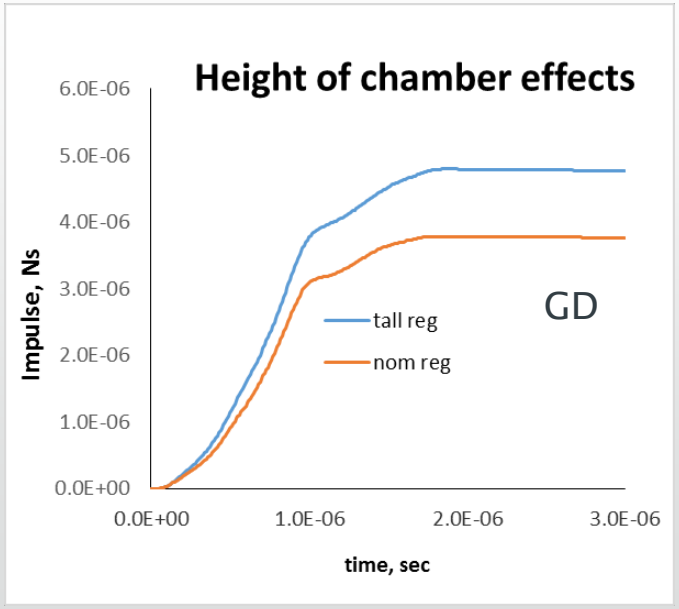


Both $I_{EM}$ and $I_{GD}$ – some increase

But $I_{EM}$ increased only in first half-cycle

Why?

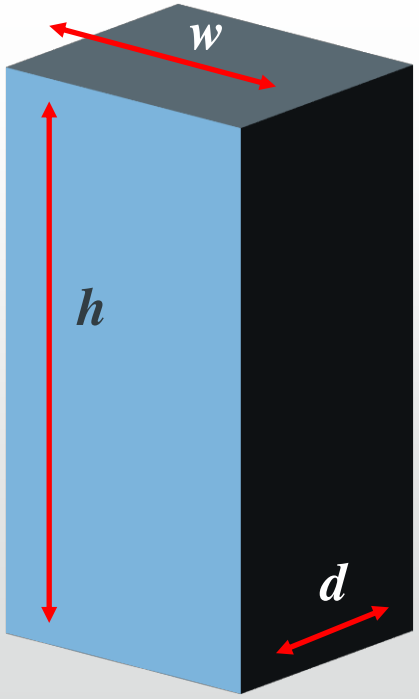

MARS SPACE LTD
SPACE AND PLASMA TECHNOLOGIES

# Height

UNIVERSITY OF Southampton
School of Electronics and Computer Science

Late ablation:
The rate is independent on height

Due to edge effects

Very short chamber?

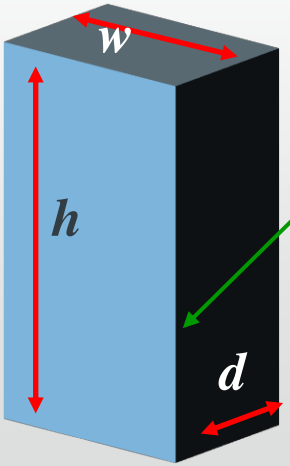


Height reduction ?
Up to a limit –
losses to electrodes

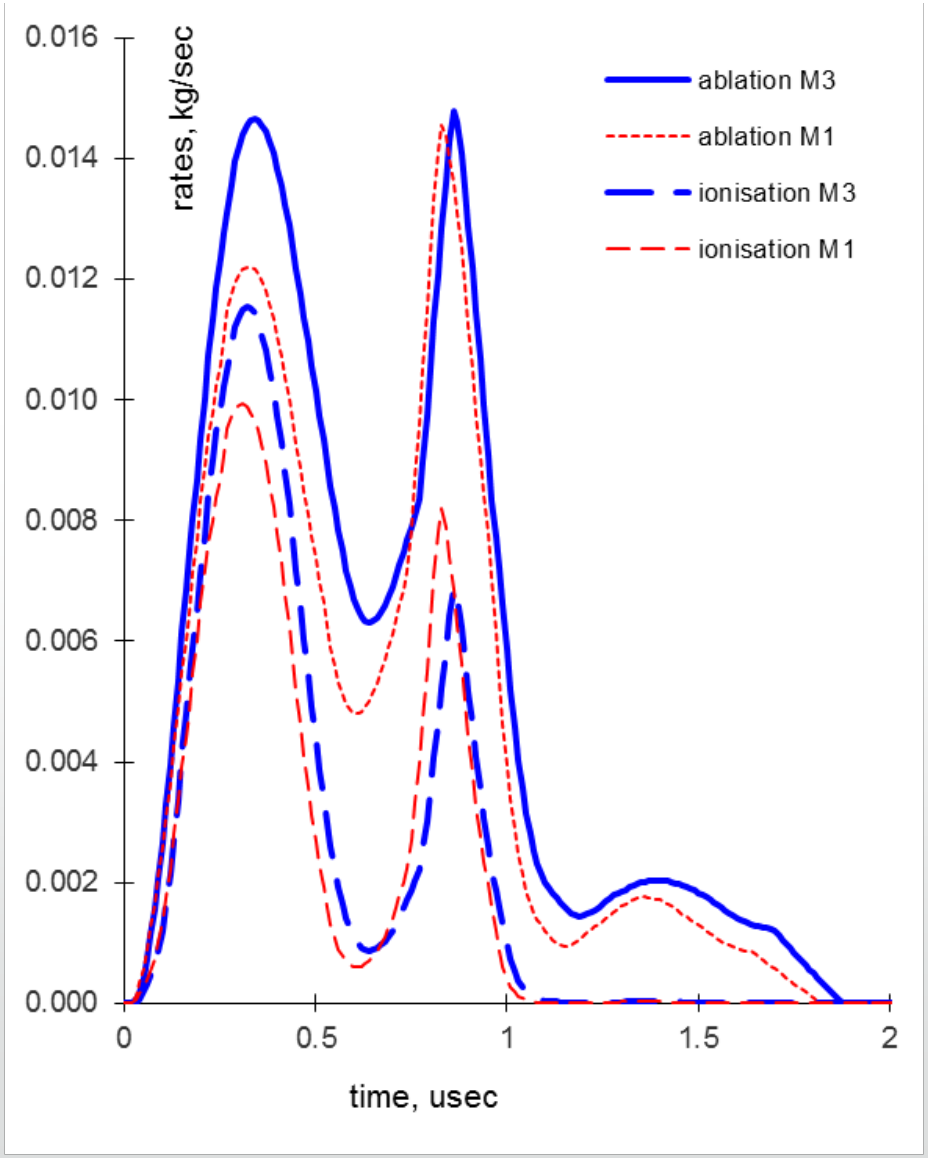

MARS SPACE LTD
SPACE AND PLASMA TECHNOLOGIES

# Scaling

UNIVERSITY OF Southampton
School of Electronics and Computer Science

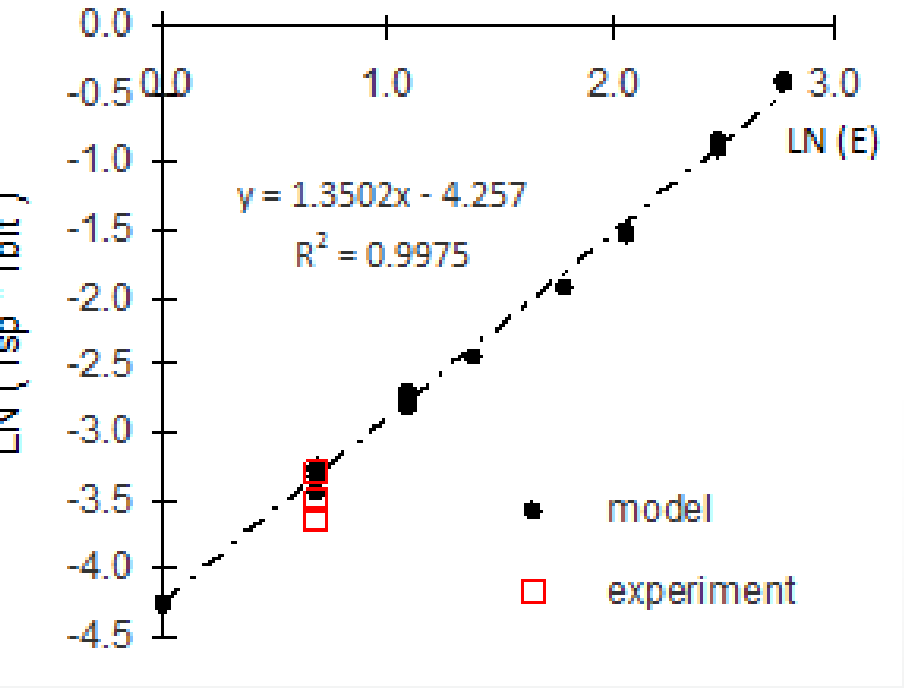


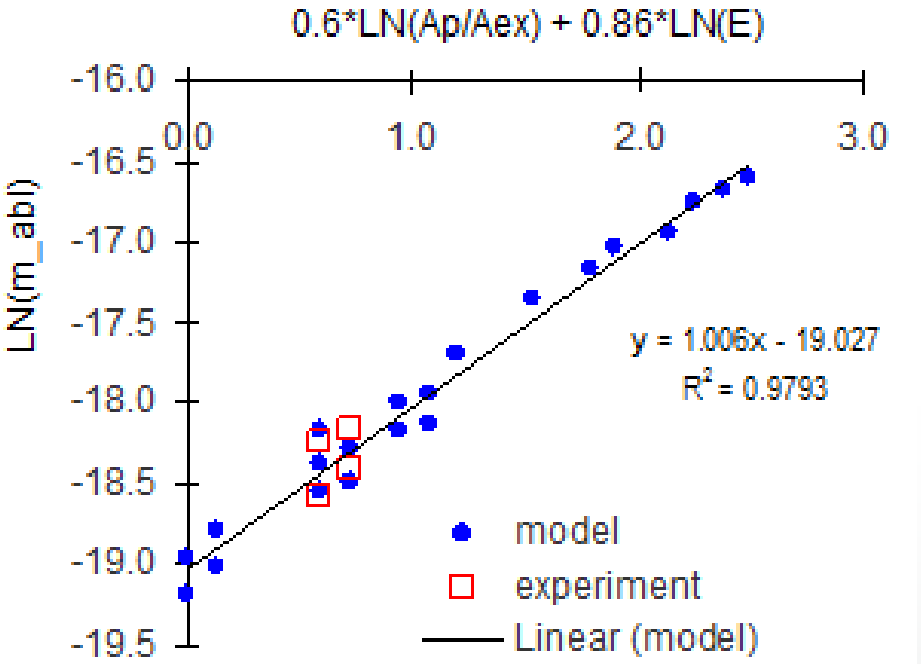


$$I_{bit} I_{sp} : E^{1.35}$$

$$m_{abl} : \left(\frac{A_p}{A_{ex}}\right)^{0.6} E^{0.86}$$

---

$$I_{bit} I_{sp} : E^{1.6}$$

R. L. Burton, P. J. Turchi, (1998)

$$m_{abl} : \left(\frac{A_p}{A_{ex}}\right)^{1.0} E^{1.0}$$

MARS SPACE LTD
SPACE AND PLASMA TECHNOLOGIES

UNIVERSITY OF Southampton
School of Electronics and Computer Science

# Summary

MARS SPACE LTD
SPACE AND PLASMA TECHNOLOGIES

# Model tool

UNIVERSITY OF Southampton
School of Electronics and Computer Science

- Simulation tool to optimise small PPTs
  - Simple and flexible
  - Needs minimal adjustment
- Allows to look at coupling between plasma phenomena and geometry
  - Effects of surface and edges
  - Guide for the design